World Academy of Science, Engineering and Technology
International Journal of Mechanical and Mechatronics Engineering
Vol:6, No:12, 2012

Dynamic Modeling of Underwater Manipulator and its Simulation

Ruiheng Li, Amir Parsa Anvar, Amir M. Anvar, and Tien-Fu Lu

***Abstract*—**High redundancy and strong uncertainty are two main characteristics for underwater robotic manipulators with unlimited workspace and mobility, but they also make the motion planning and control difficult and complex. In order to setup the groundwork for the research on control schemes, the mathematical representation is built by using the Denavit-Hartenberg (D-H) method [9]&[12]; in addition to the geometry of the manipulator which was studied for establishing the direct and inverse kinematics. Then, the dynamic model is developed and used by employing the Lagrange theorem. Furthermore, derivation and computer simulation is accomplished using the MATLAB environment. The result obtained is compared with mechanical system dynamics analysis software, ADAMS. In addition, the creation of intelligent artificial skin using Interlink Force Sensing Resistor™ technology is presented as groundwork for future work.

***Keywords*—**Manipulator System, Robot, AUV, Denavit-Hartenberg method Lagrange theorem, MALTAB, ADAMS, Direct and Inverse Kinematics, Dynamics, PD Control-law, Interlink Force Sensing Resistor™, intelligent artificial skin system.

I. Introduction

THE significance of the underwater robot lays in the potential and promising future of its application as an effective and intelligent solution for ocean-based industrial applications. A properly designed Autonomous Underwater Vehicle (AUV) should be able to carry out operations in an unstructured oceanic underwater environment while providinga real-time interface to the operator for handling the tasks. The tasks may include: diving down to search for a certain object, picking the object, manipulating the object such as opening a jar, turning a wellhead, and bring the collected items back to the surface (see Figs. 1, 2 & 3 (a), (b) & (c)).

Although the ability to operate in the subsea environment presents many opportunities and benefits in research, commercial and military endeavors, the added challenge of working underwater often results in technologies that are either very expensive or have limited functionality. The design work started from analyzing the current available various components and operating control technologies of the AUV. Then the mechanical structure is determined, including the body frame, sealing methods and gripper mechanism.

In this paper, we are going to address the kinematics model of the manipulator, as well as investigate its inverse kinematics and present, as groundwork, the creation of intelligent artificial skin using Interlink Force Sensing Resistor™ technology.

Computer simulation is conducted to verify the movement control process of the arm, through which the parameters of joint angles, locations and torques are obtained.

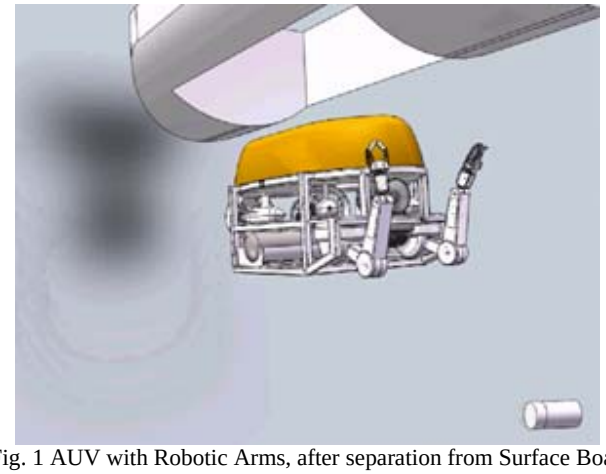

Fig. 1 AUV with Robotic Arms, after separation from Surface Boat, diving-down towards Underwater Object of Interest

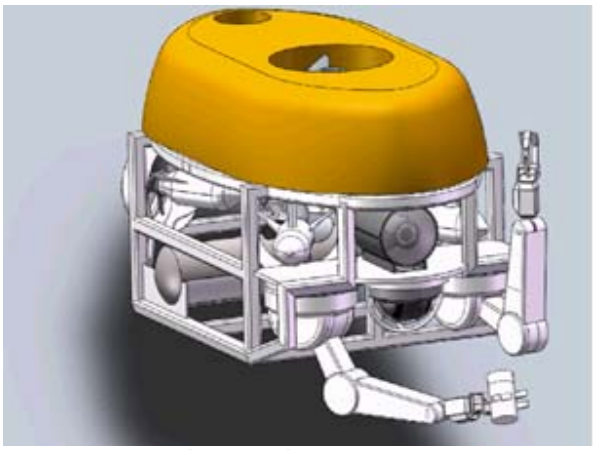

Fig. 2 Underwater Object Recovery Process

R. Li is a Post Graduate Student from School of Mechanical Engineering, the University of Adelaide, South Australia, 5005, Australia.

A.P. Anvar is a Post Graduate Student from School of Mechanical Engineering, the University of Adelaide, South Australia, 5005, Australia (e-mail: amir.p.anvar@student.adelaide.edu.au).

A.M. Anvar is with School of Mechanical Engineering, the University of Adelaide, South Australia, 5005, Australia (e-mail: amir.anvar@adelaide.edu.au).

T.F. Lu is with School of Mechanical Engineering, the University of Adelaide, South Australia, 5005, Australia (e-mail: tien-fu.lu@adelaide.edu.au).

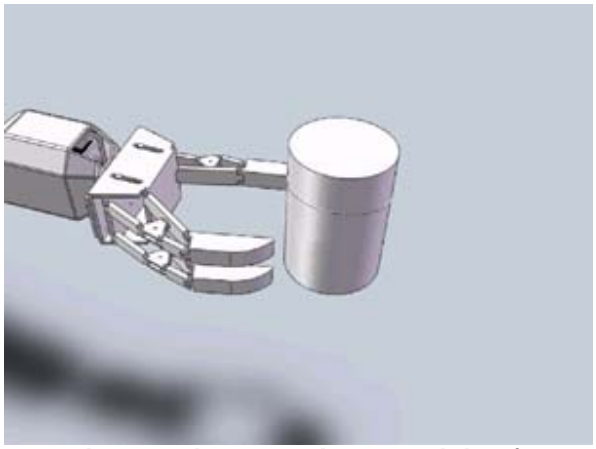

(a) Underwater Robotic Manipulator arm with three fingers

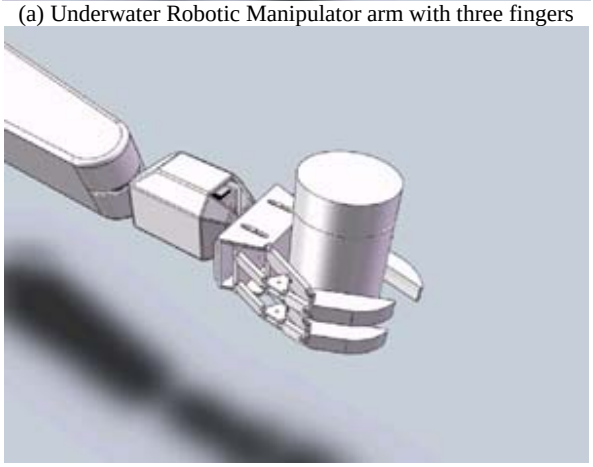

(b) Object Grasping and Manipulation Process

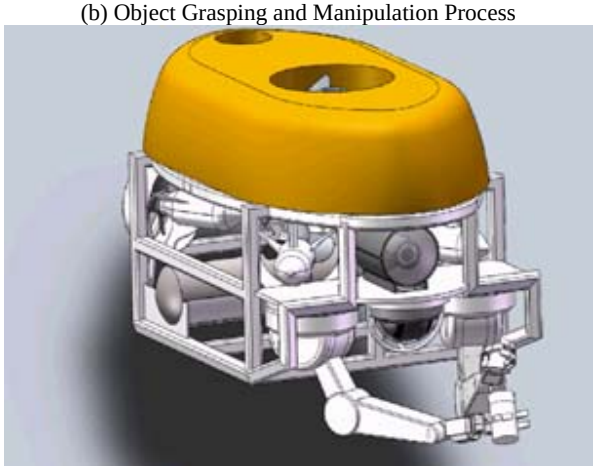

(c)

Fig. 3 Underwater Robotic Manipulation activity

II. D-H Representation of the Manipulator

Before calculations and analysis of manipulator kinematics, it is necessary to setup mathematical models for representing the positions, orientations and frames of each manipulator link. The general tool used for the space parameters is called the homogeneous transformation matrix that cans interrelatekinematical conditions within different coordinate systems. The transformation matrix in three-dimensional spaces with a size of 4 by 4, and consists of a position vector and a rotation matrix.

$$ {}^{0}T_3 = T_{01}T_{12}T_{23} = \begin{bmatrix} a_{11} & a_{12} & a_{13} & a_{14} \\ a_{21} & a_{22} & a_{23} & a_{24} \\ a_{31} & a_{32} & a_{33} & a_{34} \\ 0 & 0 & 0 & 1 \end{bmatrix} \quad (1) $$

$$ a_{11} = -s_0 $$
$$ a_{12} = -c_0c_1s_2 - c_0s_1c_2 $$
$$ a_{13} = c_0c_1c_2 - c_0s_1s_2 $$
$$ a_{14} = c_0c_1c_2L_2 - c_0s_1s_2L_2 + c_0c_1L_1 $$
$$ a_{21} = c_0 $$
$$ a_{22} = -s_0s_2c_1 - s_0s_1c_2 $$
$$ a_{23} = s_0c_1c_2 - s_0s_1s_2 $$
$$ a_{24} = s_0c_1c_2L_2 - s_0s_1s_2L_2 + s_0c_1L_1 $$
$$ a_{31} = 0 $$
$$ a_{32} = -s_1s_2 + c_1c_2 $$
$$ a_{33} = s_1c_2 + c_1s_2 $$
$$ a_{34} = s_1c_2L_2 + c_1s_2L_2 + s_1L_1 + L_0 $$

III. Trajectory Generation

Rough, jerky motions tend to cause increased wear on the mechanism and vibrations by exciting resonances in the manipulator. Therefore, it is desirable for the motion of the manipulator to be smooth. The path of the manipulator is governed by a smooth and continuous function. Furthermore, the first and second derivatives of that function are used to regulate velocity and acceleration respectively [5]. For making a signal smooth motion, a cubic polynomial and four constraints are evident. The four constraints are:

$$ \begin{cases} \theta(0) = \theta_0 \\ \theta(t_f) = \theta_f \\ \dot{\theta}(0) = 0 \\ \dot{\theta}(t_f) = 0 \end{cases} $$

where t_f is the time when the manipulator reaches its goal position,θ_0 is the initial angle position andθ_f is the goal angle position. The cubic polynomial has the form:

$$ \theta(t) = a_0 + a_1t + a_2t^2 + a_3t^3 \quad (2) $$

Then the joint velocity and acceleration along this path are:

$$ \dot{\theta}(t) = a_1 + 2a_2t + 3a_3t^2 $$
$$ \ddot{\theta} = 2a_2 + 6a_3t \quad (3) $$

Combining the two equations above with the four desired constraints yields four equations in four unknowns:

$$ \begin{cases} \theta_0 = a_0 \\ \theta_f = a_0 + a_1t_f + a_2{t_f}^2 + a_3{t_f}^3 \\ 0 = a_1 \\ 0 = a_1 + 2a_2t_f + 3a_3{t_f}^2 \end{cases} \quad (4) $$

Solving these equations, we obtain:

$$\begin{cases} a_0 = \theta_0 \\ a_1 = 0 \\ a_2 = \frac{3}{{t_f}^2}(\theta_f - \theta_0) \\ a_2 = -\frac{2}{{t_f}^3}(\theta_f - \theta_0) \end{cases} \quad (5)$$

The obtained coefficient of the polynomial can be calculated, when the joint angle position, time and desired final angle position is known (see Table I).

TABLE I
TRAJECTORY OF A DEFINED MANIPULATOR MOTION

	θ	$\dot{\theta}$	$\ddot{\theta}$
Rotary joint 1	$\frac{\pi}{100}t^2 - \frac{\pi}{1500}t^3$	$\frac{\pi}{50}t - \frac{\pi}{500}t^2$	$\frac{\pi}{50} - \frac{\pi}{250}t$
Rotary joint 2	$-\frac{\pi}{2} + \frac{3\pi}{100}t^2 - \frac{\pi}{500}t^3$	$\frac{3\pi}{50}t - \frac{3\pi}{500}t^2$	$\frac{3\pi}{50} - \frac{3\pi}{2500}t$
Rotary joint 3	$\frac{\pi}{200}t^2 - \frac{\pi}{3000}t^3$	$\frac{\pi}{100}t - \frac{\pi}{1000}t^2$	$\frac{\pi}{100} - \frac{\pi}{500}t$

For a particular case, we define the three rotary joint positions of the initial manipulator configuration. These are:

$$\theta_{10} = 0, \theta_{20} = -\frac{\pi}{2}, \theta_{30} = 0$$

The desired final positions are:

$$\theta_{1f} = \frac{\pi}{3}, \theta_{2f} = \frac{\pi}{2}, \theta_{3f} = -\frac{\pi}{6}$$

The time interval is$t_f = 10s$. By substituting the obtained coefficients in (5) into the assumed polynomial, we can define the position, velocity and acceleration of the each joint as a function of time, which have been plotted in Figs. 4, 5 and 6.

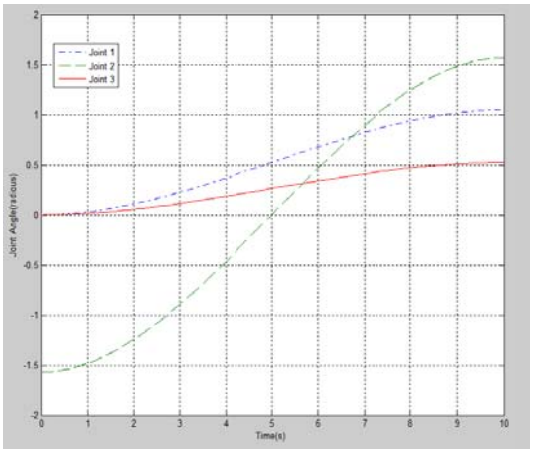

Fig. 4 Joint Displacement (radian)

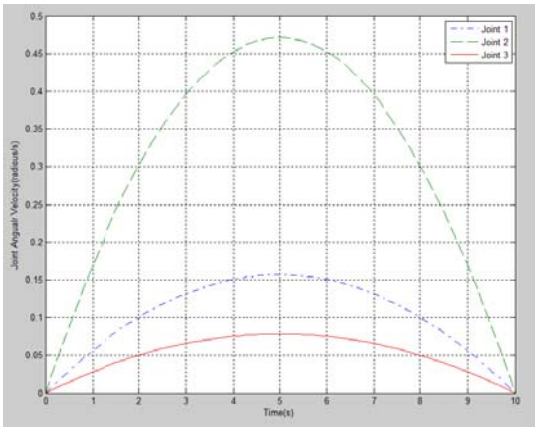

Fig. 5 Joint Angular Velocity (radian/s)

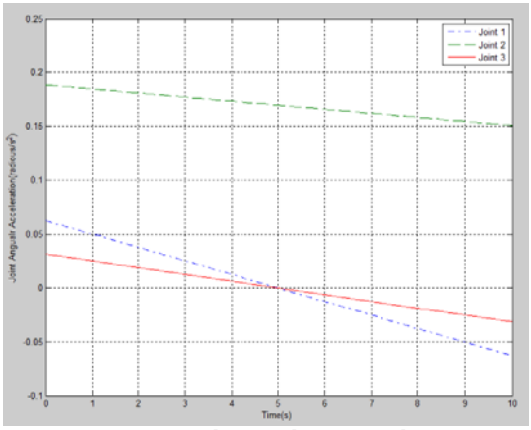

Fig. 6 Joint Angular Acceleration (radian/s^2)

IV. DYNAMICS MODEL OF MANIPULATOR

The underwater manipulator's dynamics model is established using the Lagrange method. The first step to establish the dynamics model is to choose a generalized coordinate system, using which we can determine the manipulator's geometry and the forces applied. We choose the Homogeneous Coordinate System, since it is often simpler and

more symmetric than Cartesian Coordinate Counterparts [5]. We assume that the manipulator has n degrees of freedom and consists of an n mass point system. Then each center point vector can be described in generalized coordinatesby $\vec{r}_i = \vec{r}_i(q_1, q_2 \dots q_n)$, $i = 1, 2 \dots N$. Where $q_1, q_2 \dots q_n$ are the coordinate variables. The position of a point in Homogeneous Coordinate is ${}^i\vec{r} = \begin{bmatrix} {}^ix & {}^iy & {}^iz & 1 \end{bmatrix}^T$. The change of frame from i to base zero is $\vec{r} = {}^0A_i\ {}^i\vec{r}$. A is the transformation matrix. The homogeneous speed of this point mass is defined as:

$$\dot{\vec{r}} = {}^0\dot{A}_i \cdot {}^i\vec{r} = \left(\sum_{j=1}^{i} \frac{\partial A_i}{\partial q} \dot{q}_j\right) {}^i\vec{r} \tag{6}$$

Lagrangian dynamic formulation is based on the energy-balance approach [11], so we need to get started by analyzing the potential and kinetic energies. The expression for the kinetic energy of an element i is:

$$\begin{aligned} dT_i &= \frac{1}{2}\dot{\vec{r}} \cdot \dot{\vec{r}} dm = \frac{1}{2} diag\left(\dot{\vec{r}}\dot{\vec{r}}^T\right) dm \\ &= \frac{1}{2} diag\left[\left(\sum_{j=1}^{i} \frac{\partial\ {}^0A_i}{\partial q_j}\dot{q}_j\ {}^i\vec{r}\right)\left(\sum_{k=1}^{i} \frac{\partial\ {}^0A_i}{\partial q_k}\dot{q}_k\ {}^i\vec{r}\right)^T\right] dm \\ &= \frac{1}{2} diag\left[\sum_{j=1}^{i}\sum_{k=1}^{i} \frac{\partial\ {}^0A_i}{\partial q_j}\ {}^i\vec{r}\ {}^i\vec{r}^T \frac{\partial\left({}^0A_i\right)^T}{\partial q_k}\dot{q}_j\dot{q}_k\right] dm \end{aligned} \tag{7}$$

Then the whole domain was integrated with consideration of the kinetic energy $T_i$for link i:

$$\begin{aligned} T_i &= \int_{link\ i} dT_i = \frac{1}{2} \\ &\int_{link\ i} diag\left[\sum_{j=1}^{i}\sum_{k=1}^{i} \frac{\partial\ {}^0A_i}{\partial q_j}\ {}^i\vec{r}\ {}^i\vec{r}^T \frac{\partial\left({}^0A_i\right)^T}{\partial q_k}\dot{q}_j\dot{q}_k\right] dm \\ &= \frac{1}{2} diag\left[\sum_{j=1}^{i}\sum_{k=1}^{i} \frac{\partial\ {}^0A_i}{\partial q_j}\left[\int_{link\ i}\left({}^i\vec{r}\ {}^i\vec{r}^T\right)dm\right]\frac{\partial\left({}^0A_i\right)^T}{\partial q_k}\dot{q}_j\dot{q}_k\right] = \\ &\frac{1}{2}\sum_{j=1}^{i}\sum_{k=1}^{i} diag\left[\frac{\partial\ {}^0A_i}{\partial q_j} J_i \frac{\partial\left({}^0A_i\right)^T}{\partial q_k}\right]\dot{q}_j\dot{q}_k \end{aligned} \tag{8}$$

where: $J_i = \int_{link\ i}\left({}^i\vec{r}\ {}^i\vec{r}^T\right)dm =$

$$\int_{link\ i}\begin{bmatrix} {}^ix \\ {}^iy \\ {}^iz \\ 1 \end{bmatrix}\begin{bmatrix} {}^ix & {}^iy & {}^iz & 1 \end{bmatrix} dm$$

In which the mass distribution matrix is olink i.
Mass distribution of the manipulator relative to the reference frame is defined by J_i. The mass center is C=$[x_c \quad y_c \quad z_c]^T$, the moment of inertia representing the rotational motion about three axes are I_x, I_y and I_z, and the product inertias are I_{xy}, I_{yz} and I_{xz}. Then the kinetic energy of the manipulator is:

$$\begin{aligned} T &= \sum_{i=1}^{n} T_i = \frac{1}{2}\sum_{i=1}^{n}\sum_{j=1}^{i}\sum_{k=1}^{i} diag\left(\frac{\partial\ {}^0A_i}{\partial q_j} J_i \frac{\partial\left({}^0A_i\right)^T}{\partial q_k}\right)\dot{q}_j\dot{q}_k \\ &= \frac{1}{2}\sum_{j=1}^{n}\sum_{k=1}^{n}\left[\sum_{i=max\{j,k\}}^{n} diag\left(\frac{\partial\ {}^0A_i}{\partial q_j} J_i \frac{\partial\left({}^0A_i\right)^T}{\partial q_k}\right)\right]\dot{q}_j\dot{q}_k \\ &= \frac{1}{2}\sum_{j=1}^{n}\sum_{k=1}^{n} h_{jk}\,\dot{q}_j\dot{q}_k \\ &= \frac{1}{2}\dot{q}^T H(q)\dot{q} \end{aligned} \tag{9}$$

$x_c = \frac{1}{m}\int x dm$	$y_c = \frac{1}{m}\int y dm$	$z_c = \frac{1}{m}\int z dm$
$I_x = \int (y^2 + z^2) dm$	$I_y = \int (x^2 + z^2) dm$	$I_z = \int (x^2 + y^2) dm$
$I_{xy} = \int xy dm$	$I_{xz} = \int xz dm$	$I_{yz} = \int yz dm$

where: m is the mass of a link;$\int dm = m$ for any link. The x, y and z are the position vectors of an integral element within the link body domain. The inertia tensor H_i showing the mass distribution of link i is:

$$H_i = \begin{bmatrix} \frac{-{}^iI_x + {}^iI_y + {}^iI_z}{2} & {}^iI_{xy} & {}^iI_{xz} & m_i\ {}^ix_c \\ {}^iI_{xy} & \frac{{}^iI_x - {}^iI_y + {}^iI_z}{2} & {}^iI_{yz} & m_i\ {}^iy_c \\ {}^iI_{xz} & {}^iI_{yz} & \frac{{}^iI_x + {}^iI_y - {}^iI_z}{2} & m_i\ {}^iz_c \\ m_i\ {}^ix_c & m_i\ {}^iy_c & m_i\ {}^iz_c & m_i \end{bmatrix} \tag{10}$$

Next is the process to derive the potential energy. In frame i, the mass center point position is expressed as $\tilde{r}_{ci}$, and the expression in the base zero frame is $\tilde{r}_{ci} = {}^0A_i\ {}^i\tilde{r}_{ci}$, and then the potential energy expression in frame i is:

$$V_i = -m_i\bar{g} \cdot \tilde{r}_{ci} = -m_i\bar{g} \cdot {}^0A_i\ {}^i\tilde{r}_{ci} \tag{11}$$

where: $\bar{g}$ is the gravitational acceleration vector in base zero frame. By integral within the whole domain, we get the overall potential energy of the manipulator studied.

$$V = \sum_{i=1}^{n} V_i = -\sum_{i=1}^{n} m_i\bar{g} \cdot {}^0A_i\ {}^i\tilde{r}_{ci} \tag{12}$$

The Lagrangian dynamic formulation provides a means of deriving the equations of motion from a scalar function called the Lagrangian, which is defined as the difference between the kinetic and potential energy of a mechanical system [11].

$$\begin{aligned} L &= T - V \\ \frac{\partial L}{\partial \dot{q}_j} &= \frac{\partial T}{\partial \dot{q}_j} = \sum_{k=1}^{n} h_{ij}\dot{q}_k \\ \frac{d}{dt}\frac{\partial L}{\partial \dot{q}_j} &= \sum_{k=1}^{n} h_{ij}\ddot{q}_k + \sum_{k=1}^{n} \dot{h}_{ij}\dot{q}_k \\ \frac{\partial L}{\partial q_j} &= \frac{\partial T}{\partial q_j} - \frac{\partial V}{\partial q_j} \end{aligned} \tag{13}$$

$$= \frac{1}{2}\dot{q}^T \frac{\partial H}{\partial q_i} - \left(-\sum_{i=1}^{n} m_i \bar{g}^T \frac{\partial\, {}^0A_i}{\partial q_j}\, {}^i\tilde{r}_{ci} \right)$$
$$= \frac{1}{2}\dot{q}^T \frac{\partial H}{\partial q_i}\dot{q} - g_j \tag{14}$$

In our notation, the Lagrangian of a manipulator is:

$$L(q_j, \dot{q}_j) = T(q_j, \dot{q}_j) - V(q_j)$$

The equations of motion for the manipulator are then given by:

$$\frac{d}{dt}\frac{\partial L}{\dot{q}_j} - \frac{\partial L}{q_j} = \tau$$

Substituting all the values into this equation we get:

$$\sum_{k=1}^{n} h_{ij}\ddot{q}_k + \sum_{k=1}^{n} \dot{h}_{ij}\dot{q}_k - \frac{1}{2}\dot{q}^T \frac{\partial H}{\partial q_i}\dot{q} + g_j = \tau_j \tag{15}$$

where j= 1,…, n. And rewriting the equation into matrix format:

$$H(q)\ddot{q} + \begin{bmatrix} \dot{q}^T C_1 \dot{q} \\ \vdots \\ \dot{q}^T C_n \dot{q} \end{bmatrix} + G = \tau \tag{16}$$

$C_i$is the Coriolis and centrifugal coefficient matrix.

$$H(q)\ddot{q} + C(q)\dot{q} + G(q) = \tau$$

Where:$(q) = [h_{ij}], C(q, \dot{q}) = \begin{bmatrix} \dot{q}^T C_1 \\ \vdots \\ \dot{q}^T C_n \end{bmatrix}, G(q) = \begin{bmatrix} g_1 \\ \vdots \\ g_n \end{bmatrix},$

$$\tau = \begin{bmatrix} \tau_1 \\ \vdots \\ \tau_2 \end{bmatrix}.$$

V. Kinematics Equation Derivation

In this section, we use MATLAB programming to assist us in deriving the kinematics equation of the three link underwater manipulator. The advantage of MATLAB is that it can deal with complex matrix manipulation, which will make the derivation process easier and quicker. As revealed before, the velocity of a point on the manipulator can be obtained by taking derivatives on the position functions. From the previous results, the position in terms of the homogeneous coordinates can be obtained using transformation matrix. From the value of link parameters, the individual link-transformation matrices can be computed. Then the link transformations can be multiplied together to obtain the single transformation that relates frame $[N]$ to frame[0]:

$${}^0T_{\mathrm{n}} = {}^0T_1\, {}^1T_2\, {}^2T_3 \cdots {}^{n-1}T_n = A_1A_2A_3 \cdots A_4 \tag{17}$$

For the transformation matrix of rotational joints, the partial derivative of A_i with respect to the variable $\theta_i$is determined. Therefore, we can see:

$$\frac{\partial A_i}{\partial \theta_i} = Q_i A_i$$

In the equation:

$$Q_i = \begin{bmatrix} 0 & -1 & 0 & 0 \\ 1 & 0 & 0 & 0 \\ 0 & 0 & 0 & 0 \\ 0 & 0 & 0 & 0 \end{bmatrix} \tag{18}$$

Then we take the derivative of equation (17) and denote it as U_{ij}.

$$U_{ij} = \frac{\partial\, {}^0T_n}{\partial q_i} = \frac{\partial(A_1A_2 \cdots A_j \cdots A_i)}{\partial q_i} = A_1A_2 \cdots Q_jA_j \cdots A_i \quad j \le i \tag{19}$$

$$U_{ijk} = \frac{\partial U_{ij}}{\partial q_k} \tag{20}$$

Using the dynamics equation from the Lagrangian in the previous section, we rewrite equation (19):

$$\tau_i = \sum_{j=1}^{n} D_{ij}\ddot{q}_j + \sum_{j=1}^{n}\sum_{k=1}^{n} D_{ijk}\dot{q}_j\dot{q}_k + D_i \tag{21}$$

where:

$$D_{ij} = \sum_{p=max\,(i,j)}^{n} Trace\left(U_{pj}J_pU_{pi}^T\right)$$
$$D_{ijk} = \sum_{p=max\,(i,j,k)}^{n} Trace\left(U_{pjk}J_pU_{pi}^T\right)$$
$$D_i = \sum_{p=i}^{n} -m_p g U_{pi}^T \bar{r}_p \tag{22}$$

In (21), the first section is the angular acceleration inertia, the second part is the Coriolis and centrifugal force matrix and the last part is the gravity matrix. Then, we obtain the torques i for driving the relevant joint i, when a given specified motion is required.

$$\tau_i = D_{i1}\ddot{q}_1 + D_{i2}\ddot{q}_2 + D_{i3}\ddot{q}_3 + D_{i11}\dot{q}_1^2 + D_{i22}\dot{q}_2^2 + D_{i33}\dot{q}_3^2 + D_{i12}\dot{q}_1\dot{q}_2 + \mathrm{D}_{i13}\dot{q}_1\dot{q}_3 + D_{i21}\dot{q}_2\dot{q}_1 + D_{i23}\dot{q}_2\dot{q}_3 + D_{i31}\dot{q}_3\dot{q}_1 + D_{i32}\dot{q}_3\dot{q}_2 + D_i \tag{23}$$

Because$D_{iab} = D_{iba}$, we further simplify (23) and define the control torque for joint 1:

$$\tau_1 = D_{11}\ddot{q}_1 + D_{12}\ddot{q}_2 + D_{13}\ddot{q}_3 + D_{111}\dot{q}_1^2 + D_{122}\dot{q}_2^2 + D_{133}\dot{q}_3^2 + 2D_{112}\dot{q}_1\dot{q}_2 + 2D_{113}\dot{q}_1\dot{q}_3 + 2D_{123}\dot{q}_2\dot{q}_3 + D_1 \tag{24}$$

Control torque for joint 2:

$$\tau_2 = D_{21}\ddot{q}_1 + D_{22}\ddot{q}_2 + D_{23}\ddot{q}_3 + D_{211}\dot{q}_1^2 + D_{222}\dot{q}_2^2 + D_{233}\dot{q}_3^2 + 2D_{212}\dot{q}_1\dot{q}_2 + 2D_{213}\dot{q}_1\dot{q}_3 + 2D_{223}\dot{q}_2\dot{q}_3 + D_2 \quad (25)$$

Control torque for joint 3:

$$\tau_3 = D_{31}\ddot{q}_1 + D_{32}\ddot{q}_2 + D_{33}\ddot{q}_3 + D_{311}\dot{q}_1^2 + D_{322}\dot{q}_2^2 + D_{333}\dot{q}_3^2 + 2D_{312}\dot{q}_1\dot{q}_2 + 2D_{313}\dot{q}_1\dot{q}_3 + 2D_{323}\dot{q}_2\dot{q}_3 + D_3 \quad (26)$$

VI. Hydrodynamics Effects

In order to accurately model the underwater manipulator, we need to consider the additional influences on the manipulator during motion, which are oriented from the moving incompressible fluids in the underwater environment. The hydrodynamic forces, along with the manipulator weight and payload, determine the torques for generating a motion. Therefore, for the purpose of dynamics analysis, the integration of hydrodynamic forces into the equation of motion is needed. In the following section, we used Navier-Stokes equations todetermine the hydrodynamic effects including: added mass,added Coriolis and Centripetal, drag force and buoyancy [13].

TABLE II
A List of Hydrodynamic Effects

	Effect	Origin
Added mass	Modification of the dynamic	Kinetic energy of surrounded fluid
Drag forces	Modification of the dynamic	Viscosity of the fluid
Buoyancy	No more gravity effect	Density of the fluid
Currents	Current loads	Fluid
Waves	Forced oscillations	acceleration

A. Added Mass

The added mass is generated when a rigid body moves in a fluid. The movement of the rigid body, which requires an additional force, will also accelerate the fluid. The added mass effect is normally neglected in land-based robots, since the low density of the air exerts little difference, while the water can cause much more reaction force for the same manipulator motion [13]. By approximating the manipulator as slow moving and one which has three planes of symmetry, as is common for underwater vehicles, the added mass is in the form of a 6 by 6 matrix. Based on that, the matrix form expression (27) was developed by [28] for the added mass effect:

$$M_a = M_A^T = -diag\{X_U, Y_V, Z_W, K_P, M_Q, N_R\} \quad (27)$$

For simplicity, we can approximate the geometry of the designed manipulator links as cylinders. Then we can easily obtain the mass inertia matrix for each link through the equations:

$$X_U = 0$$
$$Y_V = \rho\pi r^2 L/4$$
$$Z_W = \rho\pi r^2 L/4$$
$$K_P = 0$$
$$M_Q = \rho\pi r^2 L^3/12$$
$$N_R = \rho\pi r^2 L^3/12$$

B. Buoyancy

Buoyancy is the force that is created due to the volume of the fluid displaced by the submerged body, and it is defined as:

$$B = \rho g V$$

C. Drag Force

Drag is also known as quadratic linear friction, which is the main source of effects like potential damping, wave drift damping, skin friction and so on. The drag force exerted on the links of the manipulator will be modeled based on strip theory, which is used by replacing the surface integral with a line integral along the length of the link's cylinder. Through dividing the body surface into small elements, the force is calculated individually [13].

The drag coefficient is partially determined by the ratio between the internal forces and viscous forces. An expression was presented,in [27], for the drag coefficient:

$$\tau = -\sum_{i=1}^{n} C_d\left(\frac{l_i\theta}{D}\right) * 0.5\rho D l_i^3 dl_i|\dot{\theta}|\dot{\theta} \quad (28)$$

where:
$C_d$is the drag coefficient, which is a function of the Reynolds numbers.
D is the outer diameter of the cylinder,
$\theta$is the joint angular displacement and
$l$is the distance from the joints to the segmented length.
The Reynolds number R_n is expressed in the equation below.

$$R_n = \frac{UD}{v}$$

where:
U is the body velocity,
D is the characteristic length and
v is the water viscosity.

The hydrodynamic effects should be considered when analyzing the dynamics characteristics of the underwater manipulator. In further work, the incorporation of those effects into the equation of motion should be conducted, following the modified equation (as shown below):

$$M(q,\ddot{q}) + C(q,\dot{q}) + F(\dot{q}) + G(q) + D(q,\dot{q}) = \tau \quad (29)$$

where:
$q$is the joint angular position,
$M$is the inertia matrix,
Cdenotes the Coriolis, centrifugal forces,
Grepresents the gravity forces which include buoyancy effects,
$F$is the friction term,

*D*represents the hydraulic drag forces, which are caused by the relative velocity of the manipulator to ocean current and waves and τ is the vector of applied joint torques, which are actually control inputs.

VII. Adams Simulation

In this investigation, computer simulation is conducted for verifying the movement control process of the arm, through which the parameters of joint angles, locations and torques are obtained.

The AUV model is simplified and values are assigned for the simulation. The initial position of the underwater vehicle (robot) is in the coordinate origin (0, 0), and it is assigned an acceleration of 0.3m/s^2 along the X direction, and 0.05m/s^2 along Y direction. The joint between the main body and upper arm is assigned 5d/s^2 for angular acceleration and the joint between the upper and lower arm is assigned 10d/s^2.

In the defined motion process, the real-time position, velocity, acceleration and torques of each joint are indicated within Figs. 7 to 19.

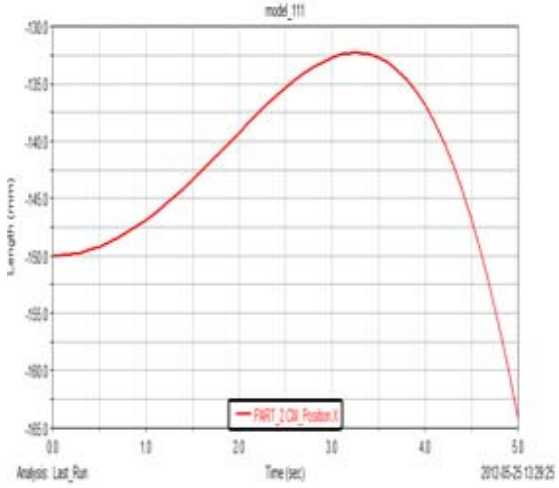

Fig. 7 Part 2 CM Position X, Length (mm) versus Time (s)

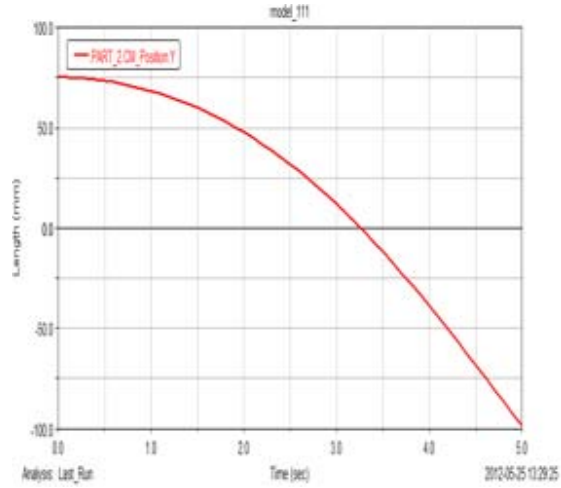

Fig. 8 Part 2 CM Position Y, Length (mm) versus Time (s)

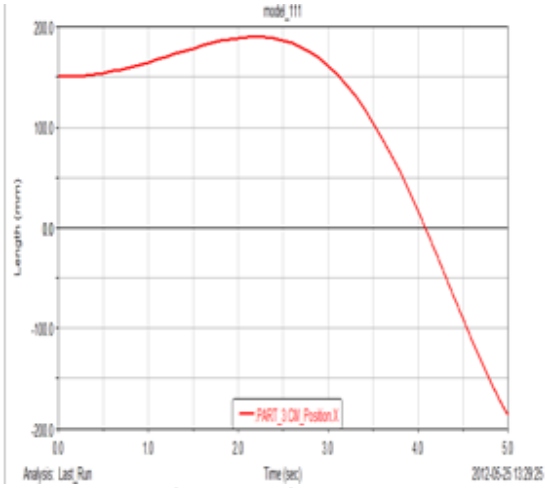

Fig. 9 Part 3 CM Velocity X, Velocity (mm/s) versus Time (s)

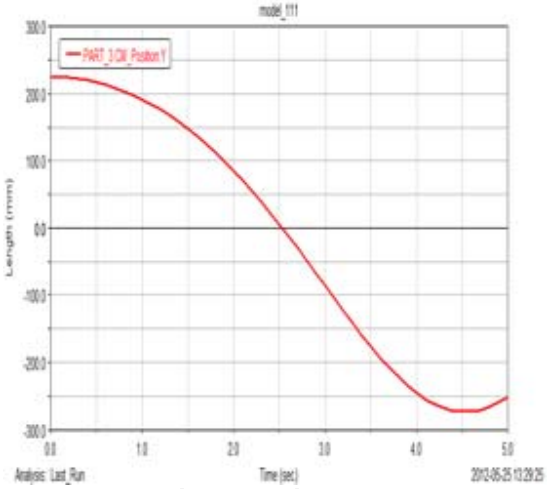

Fig. 10 Part 3 CM Velocity Y, Velocity (mm/s) versus Time (s)

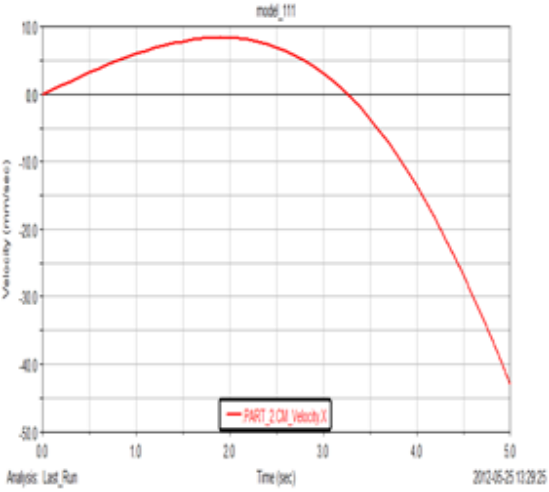

Fig. 11 Part 2 CM Velocity X, Velocity (mm/s) versus Time (s)

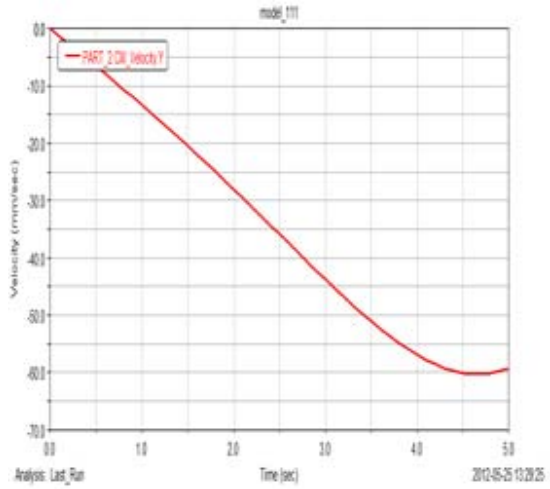

Fig. 12 Part 2 CM Velocity X, Velocity (mm/s) versus Time (s)

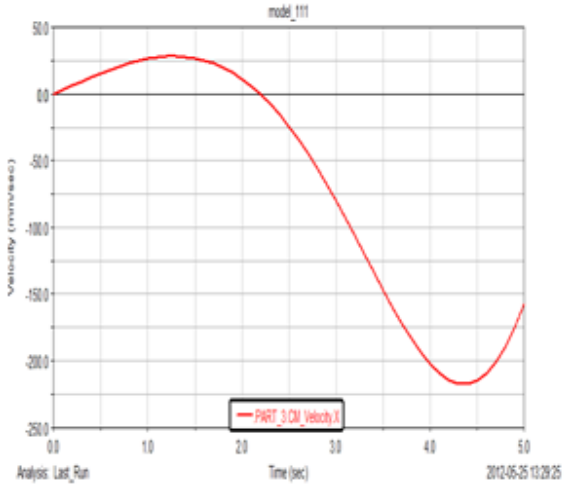

Fig. 13 CM Velocity X, Velocity (mm/s) versus Time

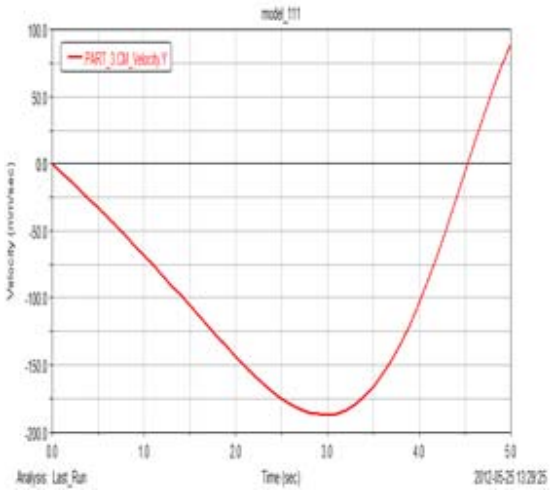

Fig. 14 Part 3 CM Velocity X, Velocity (mm/s) versus Time (s)

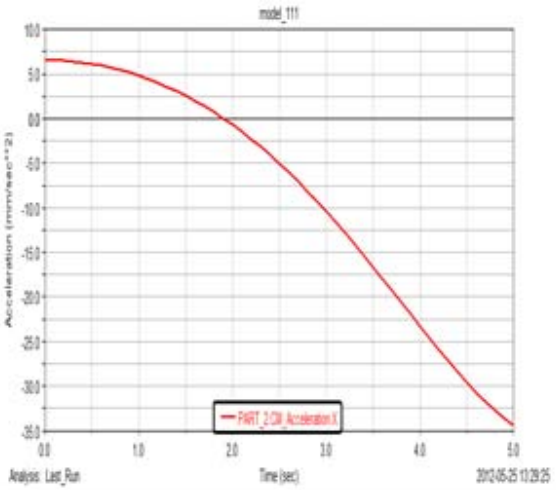

Fig. 15 Part 3 CM Velocity X, Velocity (mm/s^2) versus Time (s)

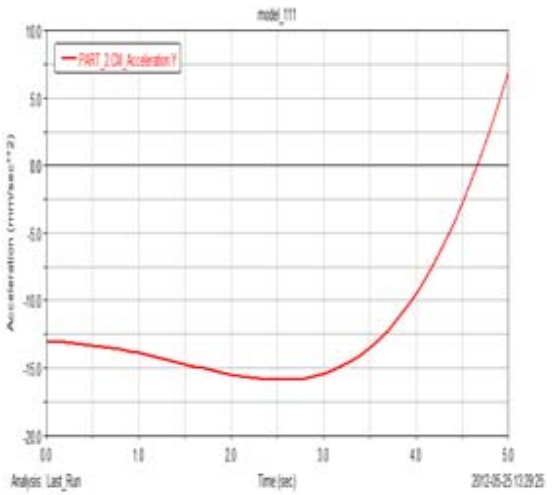

Fig. 16 Part 2 CM Acceleration X, Acc. (mm/s^2) versus Time (s)

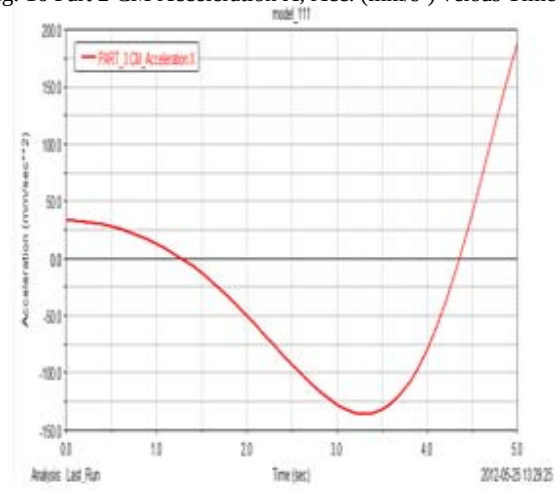

Fig. 17 Part 3 CM Acceleration X, Acc. (mm/s^2) versus Time (s)

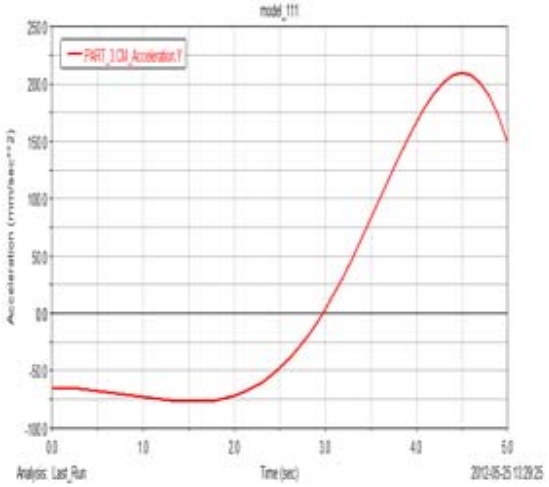

Fig. 18 Part 3 CM Acceleration X, Acc. (mm/s^2) versus Time (s)

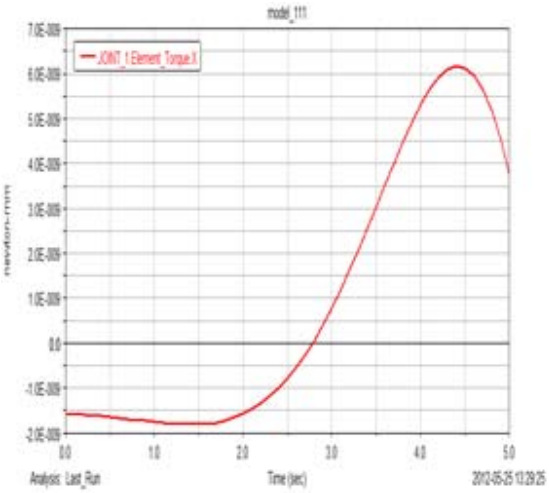

Fig. 19 Joint 1 Element Torque X, Newton (mm) versus Time (s)

VIII. Artificial Skin

Interlink Force Sensing Resistor^{TM}s(FSRs), shown in Fig. 20, may be used as the touch sensor of artificial skin for this underwater robotic manipulator arm. They may specifically be attached to the fingers for gripping force control. This would be beneficial for applying the ideal amount of force,in the underwater robotic manipulation activity illustrated in Fig. 3, to open the container without deforming it. It would also be used to repair damage in naval vessels and submarines and in many other underwater robotic manipulation applications.

Fig. 20 0.2 Inch Interlink Force Sensing Resistor 400
Source: [25]

The structure of this sensor can be seen in Fig. 21. It consists of two membranes and a spacer. The job of the spacer is to adhere and separate the membranes from one another such that they are combined with an air gap in between. The bottom membrane is made up of two traces on tails with an interdigitated array of fingers in between. The outer layer of the top membrane is an FSR^{TM} carbon based-ink. When the sensor is pressed, the upper membrane makes contact with the bottom membrane and the ink connects the two traces together. The resistance of this connection is dependent upon the applied force [26].

The force sensing characteristic of this sensor can be seen in Fig. 22. As can be seen, the sensor resistance decreases with increasing applied force. For the majority of this region the governing relationship is an inverse power law[26].This special region can be exploited by interfacing the sensor with the onboard AUV PC/104 brain via an ADC.

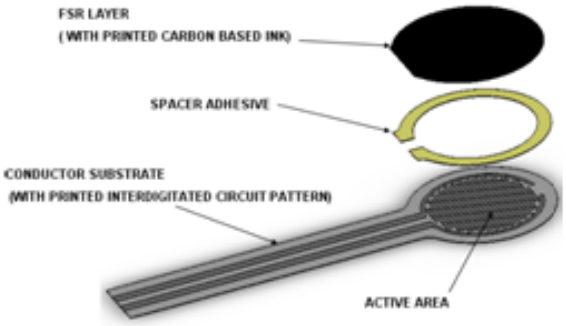

Fig. 21 Basic components of an Interlink FSR
Source: [26]

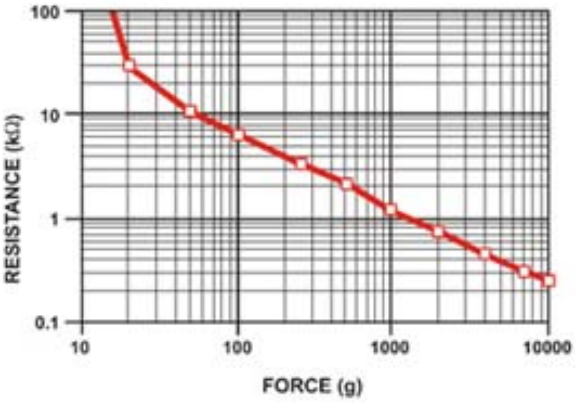

Fig. 22 Typical Force Curve of an InterlinkFSR 400
Source: [25]

IX. Conclusion

In order to setup the groundwork for the research on control schemes, the geometry of the manipulator is studied for establishing the direct and inverse kinematics. Then, the dynamic model is built by using the Lagrange theorem and modeled in MATLAB. The challenges in designing an underwater manipulator is studied which lays a foundation for integrating the hydrodynamic effects into the normal manipulator dynamics. The outcome of this research-investigation, (mainly dynamics analysis) is successfully simulated using mechanical system simulation software ADAMS. Furthermore the groundwork for future work involving the creation of intelligent artificial skin using Interlink Force Sensing Resistor^{TM} technology is presented.

REFERENCES

[1] Andrew, T 1992, Design Issues for Underwater Manipulator Systems, Department of Mechanical Engineering, University of Technology, Loughborough, Leicestershire.
[2] Anthony, M 2008, The Maritime Engineering Reference Book: A Guide To Ship Design, Construction and Operation, Elsevier USA.
[3] Bahleda, M 2002, Remotely Operated Vehicle (ROV) Technology: Applications and Advancements at Hydro Facilities, HCI Publications, California.
[4] Bruno, S &Oussama, K 2007, Springer Handbook of Robotics, Springer, Berlin.
[5] Craig, John, J 2005, Introduction to Robotics: Mechanics and Control, Upper Saddle River.
[6] Christopher von, A 2003, Autonomous Underwater Vehicles, Woods Hole Oceanographic Institution.
[7] Christ, D &Wernli, L 2007, TheROv Manual: A User Guide for Observation Class Remotely Operated Vehicles.
[8] Dana, Y, Hagen, S & David, D 1991, Design and Performance Evaluation of an Actively for Full-Ocean Depth, Department of Applied Ocean Physics and Engineering Woods Hole Oceanographic Institution.
[9] Denavit J. and Hartenberg, R.S. 1955, "A kinematic notation for lower-pair mechanisms based on matrices." *Trans ASME J. Appl. Mech,* 23:215–221.
[10] Gere, J & Timoshenko, S 1999, Mechanics of Materials, 3rdEdn, DuaHua Printing Press Co., Hong Kong.
[11] Gianluca, A 2006, Underwater Robots: Motion and Force Control of Vehicle-Manipulator Systems, Springer-Verlag, Berlin Heidelberg.
[12] Hartenberg, R. S., and Denavit J. 1964, Kinematic Synthesis of Linkages. New York: McGraw-Hill, on-line through KMODDL.
[13] IrfanAbd, R, Surina Mat S &Mohd Rizal, A 2007, Theory and Design Issues of Underwater Manipulator, International Conference on Control, Instrumentation and Mechatronics Engineering (CIM'07), Malaysia.
[14] Jee-Hwan, R & Dong-Soo, K 2001, Control of Underwater Manipulators Mounted on an ROV Using Base Force Information, International conference on Robotics & Automation.
[15] J. YUH, 2000, Design and Control of Autonomous Underwater Robots: A Survey, Kluwer Academic Publishers, Netherlands.
[16] Koray, K 2007, Modelling and motion Simulation of an Underwater Vehicle, Middle East Technical University.
[17] Louis, A 2004, Design, Modelling and Control of an Autonomous Underwater Vehicle, The University of Western Australia.
[18] Lauren, C 2006, Development of a Low-cost Underwater Manipulator, Massachusetts Institute of Technology.
[19] Michel, B, Ryan, F, Philip, R & Amelia, S 2010, Latis II Underwater remotely Operated Vehicle Technical Report, University of Maine.
[20] Miles, P & Carroll, T 2002, Build your Own Combat Robot, McGraw-Hill, Newyork.
[21] Roy, B & Louis, R 1998, Concepts in Submarine Design, Cambridge University Press, United Kingdom.
[22] Rui, G, Alexandre, S, Sergio, F, Alfredo, M, Joao, S& Fernando, P, A New ROV Design: Issues On Low Drag AND Mechanical Symmetry, Underwater Systems and Technology Laboratory, Porto.
[23] Sabiha, W & Pushkin, K 2011, Autonomous Underwater Vehicles: Modeling, Control Design, and Simulation, CRC Press, New York.
[24] Lagrange theorem. 2010, viewed July 1 2012,<http://www.slideshare.net/troywoo/rev-chapter-4-mar23rd>.
[25] Interlink Electronics 2010, *FSR 400 Data Sheet*, viewed September 3 2012, <http://www.trossenrobotics.com/productdocs/2010-10-26-DataSheet-FSR400-Layout2.pdf>.
[26] Interlink Electronics 2010, Interlink ElectronicsFSR™Force Sensing Resistors™ Integration Guide, viewed September 42012, <http://akizukidenshi.com/download/ds/interlinkelec/94-00004+Rev+B%20FSR%20Integration%20Guide.pdf>.
[27] Timothy, WM, and Stephen MR 1998, 'Development and Experimental Validation of an Underwater Manipulator Hydrodynamic Model', The International Journal of Robotics Research, vol. 17 no. 7, 748-759, viewed 3 July 2012, <http://www.stanford.edu/group/arl/cgi-bin/drupal/sites/default/files/public/publications/McLainR%2098.pdf>.
[28] Fossen, TI 2002, *Marine Control Systems, Guidance, Navigation, and Control of Ships, Rigs and Underwater Vehicles. Marine Cybernetics*, Trondheim, Norway.